Study of the Influence of Buildings on the Performance of Micro Wind Turbines in Urban Environments through Computational Simulations

Ana Carolina Finotti Azeredo[1], Andreia Aoyagui Nascimento[1 2]

[1]*School of Electrical, Mechanical, and Computer Engineering, Federal University of Goiás Av. Esperança, s/n, Campus Samambaia, Al. Ingá, Prédio B5 Eng. Mecânica, CEP: 74.690-900 - Goiânia – Goiás, Brasil*
carolazeredo@gmail.com
[2]*Center of Excellence in Hydrogen and Sustainable Technologies, Federal University of Goiás Parque Tecnológico Samambaia, Campus Samambaia, Rodovia R2, n. 3.061, CEP: 74.690-631,- Goiânia – Goiás, Brasil*
aanascimento@ufg.br

Abstract. In urban environments where space is constrained, micro wind turbines can be mounted on rooftops or nearby structures. The study of flow around cylinders adjacent to a flat surface is critical for understanding how the presence of buildings influences the performance of these micro wind turbines and optimizing their operation in urban settings. This research employs the Pseudospectral Fourier method, coupled with the Immersed Boundary method, to simulate the flow around a circular-based cylinder positioned near a wall. The simulations investigate the effect of local Reynolds number variations introduced by the wall, as well as the impact of the cylinder-to-wall gap (referred to as 'GAP') on vortex shedding behavior. The results are compared against both experimental and numerical findings from previous studies

Keywords: Pseudospectral Method; Flow around Cylinder Near Wall; Micro Wind Turbines

1 Introduction

Renewable energy sources are gaining increasing importance in Brazil, with widespread adoption due to their numerous benefits and applications. Among these, wind energy stands out, utilizing wind turbines to convert wind power into electrical energy. Wind turbines are typically classified into two main types: horizontal-axis wind turbines (HAWT), Fig. 1(a), and vertical-axis wind turbines (VAWT), Fig. 1(b) and (c). As outlined by ANEEL [1], wind turbines are categorized by capacity as small-scale (up to 500 kW), medium-scale (500–1000 kW), and large-scale (above 1000 kW).

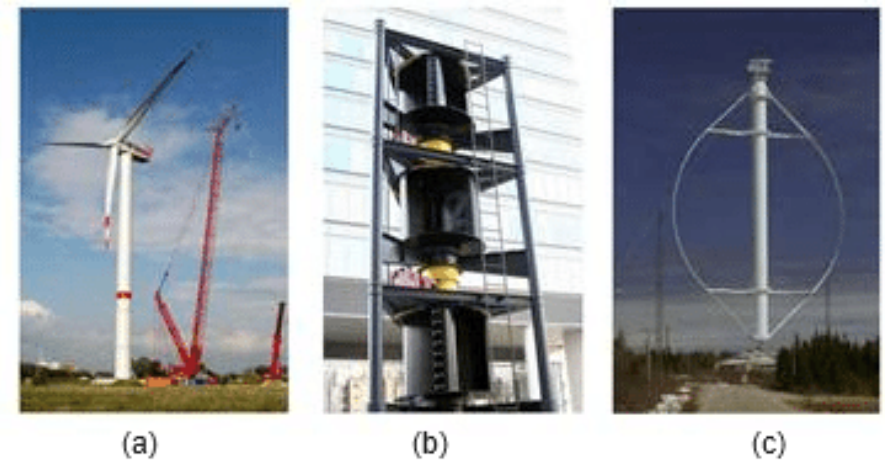

Figure 1. (a) Horizontal axis based high speed wind turbine (b) Savonius (c) Darrieus; [2].

Perea-Moreno et al. [3] demonstrated in their study that between 1977 and 2017, the scientific community conducted extensive research on renewable energy generation in urban areas. For their analysis, the authors used the Scopus Elsevier database, which allowed them to identify key research contributors, including countries such as China, the United States, the United Kingdom, Italy, Germany, and India.

In 2021, Peacock et al. [4] conducted an experimental investigation into the carbon savings potential of small wind turbines and their feasibility for integration into existing residential buildings. One of the primary objectives of the project was to identify strategies for achieving a 50% reduction in CO2 emissions from the existing housing stock in the UK by 2030. The study concluded that, akin to other microgeneration technologies, a significant portion of the microturbine's generated power may not be immediately consumed by the residence but will be exported. This export of electricity has the potential to contribute to a reduction in CO2 emissions associated with the technology.

Bassi et al. [5] reported that tall buildings in urban areas are ideal sites for installing small wind turbines (SWTs). Their article describes the installation of a horizontal-axis wind turbine (HAWT) at the Institute of Energy and Environment of the University of São Paulo. The study presented results including assessments of power quality at the grid connection point, rotor speed, wind speed, and energy production statistics. This data provides valuable insights into the operation of small wind turbines (SWTs) and can serve as input for further studies on SWT performance.

TeCSol [6] introduces the innovative Wind My Roof project, as shown in Fig.2, implemented at the Capricorne building in Rouen, France. This pioneering initiative integrates wind and solar energy using Windbox units—compact devices that capture updraft winds and sunlight to generate electricity. The project aims to optimize energy production and significantly reduce carbon emissions and energy costs for residents, thereby fostering both environmental and social benefits

Figure 2. Wind My Roof project TeCSol

In an urban environment with diverse building heights, including skyscrapers, houses, and other structures, this study utilized a simplified model to represent the physical phenomena by employing a cylinder adjacent to a wall. In this context, the cylinder represents a Savonius micro-turbine, while the wall simulates the adjacent building where the turbine is installed. The objective of this study is to understand the flow dynamics around a Savonius micro-turbine for urban applications. The chosen methodology is IMERSPEC2D, which integrates the pseudospectral Fourier method with the immersed boundary method.

2 Metodology

2.1 Mathemathical model

For the differential analysis of fluid motion, two fundamental principles must be considered: the Conservation of Mass, expressed by Eq.1, and the Conservation of Momentum, described by Eq.2, both derived from Newton's Second Law. The Navier-Stokes equations govern fluid flow dynamics, enabling the determination of velocity and pressure fields.

$$\frac{\partial u_j}{\partial x_j} = 0 \tag{1}$$

$$\frac{\partial u_j}{\partial t} + \frac{\partial (u_i u_j)}{\partial x_j} = -\frac{1}{\rho}\frac{\partial P}{\partial x_i} + \nu\Big(\frac{\partial^2 u_i}{\partial x_j^2 \partial x_j^2}\Big) + \frac{1}{\rho} f_i \tag{2}$$

where u_i represents velocity, t is the time variable, P is the pressure variable, ν is viscosity, ρ is density, and f_i , Eq.3 is the source term of the equation (in this term is possible to introduce the IBM).

$$f_{ij} = \begin{cases} F_i(x_k, t) & \text{se } x = x_k \\ 0, & \text{se } x \neq x_k \end{cases} \tag{3}$$

The Immersed Boundary Method (IBM) utilizes two distinct domains: the Lagrangian Γ and the Eulerian Ω as illustrated in Figure Figure 3. The Lagrangian domain models the immersed surface, while the Eulerian domain represents the surrounding fluid

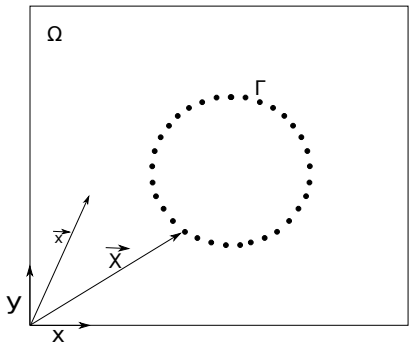

Figure 3. Diagram of the Immersed Boundary Method.

2.2 Fourier Pseudospectral Method

The solution of the Navier-Stokes equation uses to the pseudospectral Fourier method involves transforming the equation into spectral space. As a result, the formulation of the horizontal velocity field can be expressed as shown in Eq.4.

$$\frac{\partial \widehat{u_j}}{\partial t} + ik_j(\widehat{u_i * u_j}) = -\iota k_i \widehat{P} + \nu k^2 \widehat{u_i} + \widehat{f_i} \tag{4}$$

where k is the wave number, $\widehat{u_i}$ is the velocity vector transformed, ι is the complex number $\sqrt{-1}$ and f_i is the source term . The $(\widehat{u_i * u_j})$ is the non-linear term, that is solved by applying the Fourier Pseudospectral method Canuto [7]. In the transformation of Eq.1, is expressed by Eq. 5, which define the plane π, i.e., zero divergences plan [8].

$$\iota k_j \widehat{u_j} = 0 \tag{5}$$

In addition to choosing the Immersed Boundary (IB) method, another crucial requirement for Computational Fluid Dynamics (CFD) simulations is the number of grid points in the domain. The IMERSPEC development at FORTRAN achieves better accuracy when the number of nodes is equivalent to 2^N, where N is an integer. For this reason, simulations in the present study were conducted using grid points of 512x256. The time-advanced method is the fourth-order, 6-step Runge-Kutta method was employed by Nascimento et al. [8] and the dimensionless final, $t^\star = t\frac{U_\infty}{D} = 148$.

2.3 Physical Problem

The physical problem consists of a circular cross-section cylinder, $D = 1,610^{-2}m$ next fixed to the bottom wall. The modeled system is depicted in Figure 4, where the buffer zone, ZB, with a length of $5.6D$, functions as a flow filter. The forcing zone, ZF, starting at the end of the buffer zone, has a length of $2.4D$ along the horizontal axis. Exactly $53D$ in the x-direction after the forcing zone is the center of the cylinder. The wall governing the problem begins at the point $10.5D$ along the horizontal axis.

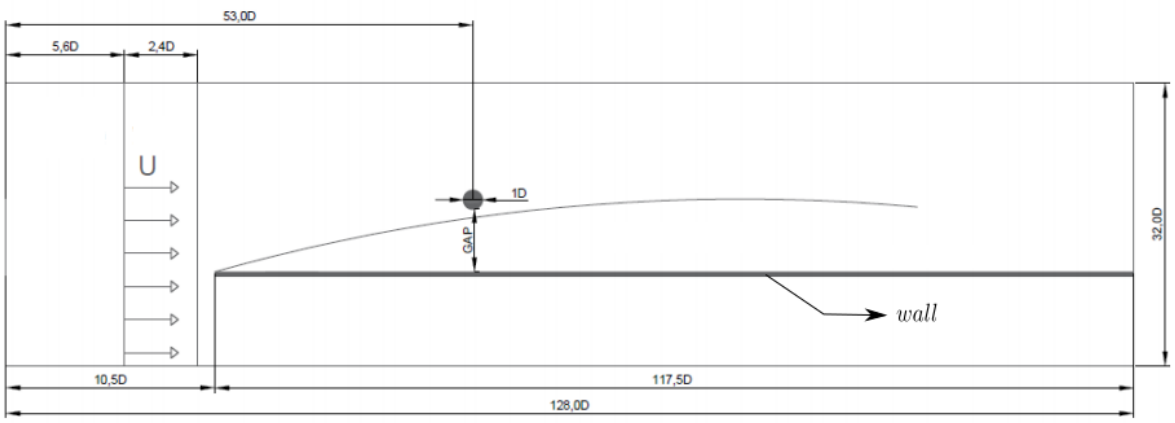

Figure 4. The size of the computational domain.

The Reynolds number, $Re_x = \frac{UL_\delta}{\nu}$, is equal to 8500, ν is the kinematic viscosity of the fluid and L_δ=42.5D. The values adopted for these properties are also provided in Table 1. That being said, the flow is considered laminar.

Table 1. System Specifications

Symbol	Description	Value
U	Maximum velocity at the duct inlet [m/s]	1.0
ρ	Fluid density [kg/m3]	1000
L_x	Dimensionless length of the domain	128 D
L_y	Dimensionless height of the domain	32.0 D
L_b	Dimensionless length of the Buffer Zone	5.6 D
L_f	Dimensionless length of the forcing zone	2.4D
GAP	distance between the cylinder and the wall	5D; 2D; 1D; 0,5D

This study also presents the frequency of vortex shedding, n, can be related to the characteristic dimension of the solid body, d, and the free-stream velocity, U. This relationship is quantified by the Strouhal number, St, which is a dimensionless parameter used to describe the frequency of vortex shedding relative to these variables. Specifically, the Strouhal number is defined as,

$$St = \frac{n \cdot d}{U}. \tag{6}$$

This equation highlights how the frequency of vortex shedding, characteristic dimension of the body, and free-stream velocity interact to influence the vortex dynamics around the body.

3 Results

Figure 5 depicts the vorticity field for flow over a cylinder with a wall distance Gap=5D, where counter-rotating vortices are illustrated, with black indicating clockwise rotation and white indicating counterclockwise rotation. It is observed that a separation zone forms at the rear of the cylinder, generating wake vortices due to flow separation from the surface, suggesting minimal influence of the flat wall boundary layer geometry at this distance.

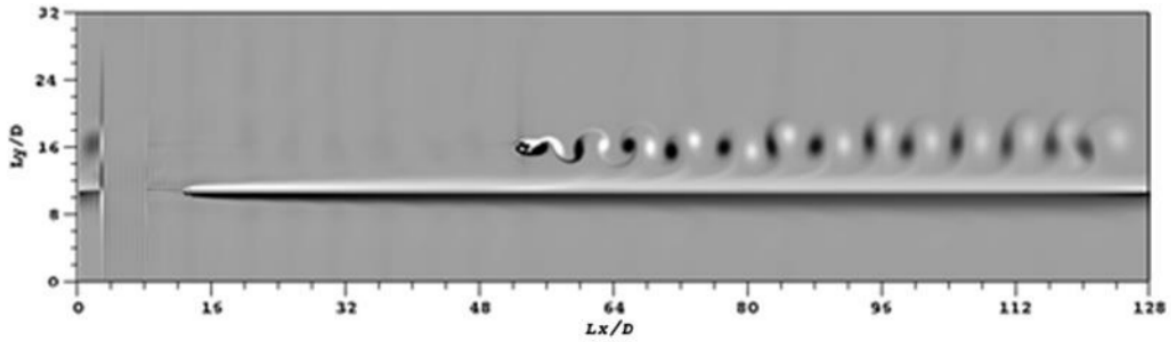

Figure 5. The size of the computational domain.

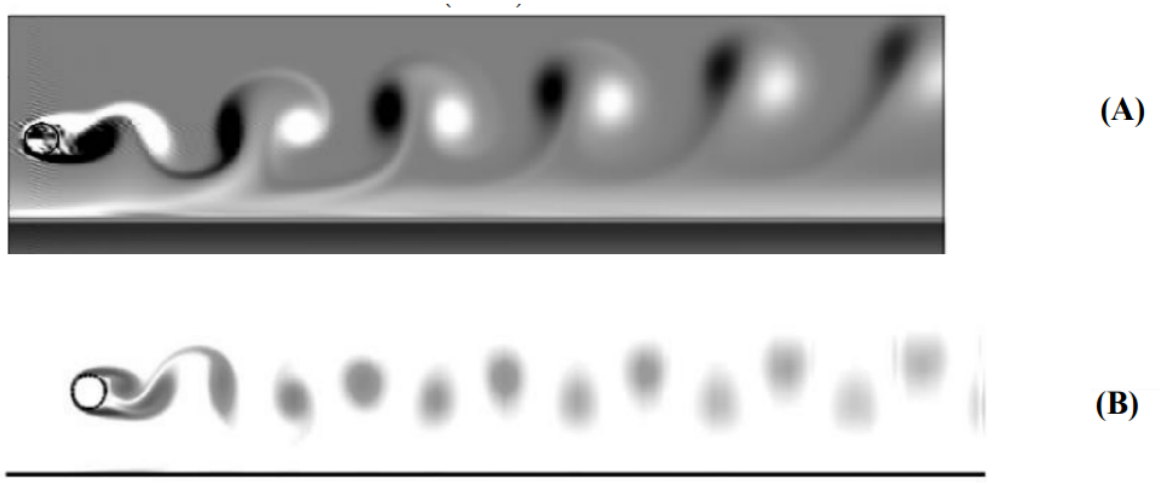

Figure 6. Flow over cylinder, Gap=2D, (A) Own work and (B) RAO et al. (2013)

Moving the cylinder closer to the wall, Gap=2D, Figure 6(A), at a dimensionless time of $t^{\star}$=100, $Re_x = 8500$, it is possible to observe that the wake pattern downstream of the cylinder is modified compared to Fig. 6. This occurs because the closer proximity of the cylinder to the wall results in an interaction between the boundary layers of these bodies. In this case, since the boundary layer of the wall has a thickness of 2.31D, the clockwise vortices, depicted in white, introduce rotational velocity within the boundary layer of the wall. Comparing Fig. 6(A) with Figure 6(B), it is also noted that there is similarity in the wake vortex shedding patterns up to the first five pairs of vortices.

Plotting the vortex contours, Fig. 7, provides a clearer understanding of their direction, as well as small recirculations near the wall regions that can alter the flow velocity. HARICHANDAN and ROY [10] also plotted the vortex contours for Gap=2D, Fig. 7(B). Analyzing both contours reveals that similar behavior is observed in the first five pairs of vortices.

In Table 2 are the Strouhal numbers with their respective gaps, showing that the values obtained in this study were close to those of the reference. It is noteworthy that the highest Strouhal number occurred when Gap=1D, while the lowest Strouhal number occurred for the smallest simulated gap value. Thus, when the cylinder was very close to the wall, there was a tendency for a lower frequency of vortex shedding.

4 Conclusions

The use of a simplified model of a cylinder near a wall to understand the flow over a Savonius microturbine installed in urban environments leads to the following conclusions:

1) With fewer fluctuations in aerodynamic force on the blades, a lower Strouhal frequency can result in a more stable aerodynamic load and consequently less structural fatigue over time.

2) A lower Strouhal number can contribute to more stable turbine operation under varying wind conditions,

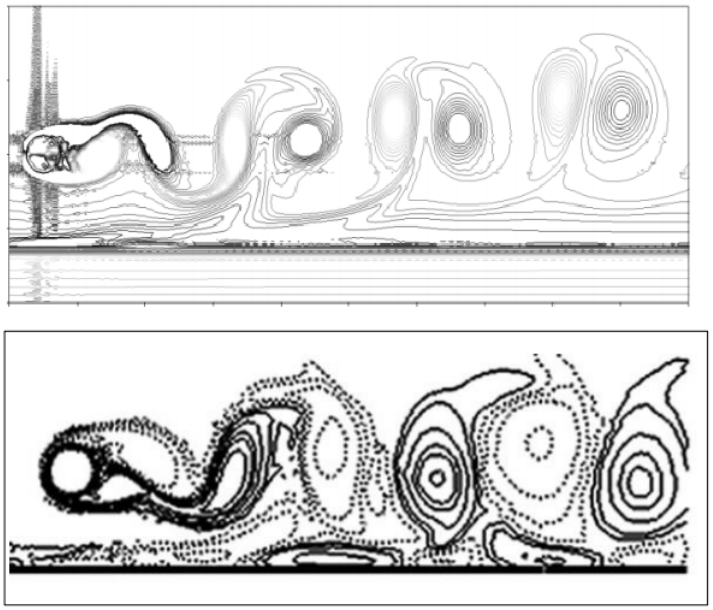

Figure 7. Flow over cylinder Gap=2D, (A) Own work and (B) HARICHANDAN and ROY (2012).

Table 2. Strouhal number for different gap values

Author	GAP	St
Present work	5D	0,2300
	2D	0,2139
	1D	0,223
	0,5D	0,198
RAO et al. (2013)	5D	-
	2D	0,2000
	1D	0,210
	0,5D	0,190

maintaining relatively constant efficiency.

3) A lower St generally leads to more stable operation of the Savonius turbine across a range of wind conditions, ensuring more consistent energy production over time, thus making it more suitable for installation in urban areas.

4) It is important to note that no filtering function was applied during the course of this study. All results were obtained without the use of any filtering techniques, ensuring that the data presented reflects the raw output of the simulations.

Acknowledgements. The authors thank Eletrobras/FURNAS and the Research and Technological Development Program (P& D) of ANEEL for the infrastructure and financial support provided for this work.

Authorship statement. This section is mandatory and should be positioned immediately before the References section. The text should be exactly as follows: The authors hereby confirm that they are the sole liable persons responsible for the authorship of this work, and that all material that has been herein included as part of the present paper is either the property (and authorship) of the authors, or has the permission of the owners to be included here.

References

[1] ANEEL. Energia Eólica. Accessed: 2024-07-11, 2019.

[2] M. Saad. Comparison of horizontal axis wind turbines and vertical axis wind turbines. *IOSR Journal of Engineering*, vol. 4, pp. 27–30, 2014.
[3] M.-A. Perea-Moreno, Q. Hernandez-Escobedo, and A.-J. Perea-Moreno. Renewable energy in urban areas: Worldwide research trends. *Energies*, vol. 11, n. 3, 2018.
[4] A. Peacock, D. Jenkins, M. Ahadzi, A. Berry, and S. Turan. Micro wind turbines in the uk domestic sector. *Energy and Buildings*, vol. 40, n. 7, pp. 1324–1333, 2008.
[5] W. Bassi, A. Rodrigues, and I. Sauer. Dataset on scada data of an urban small wind turbine operation in são paulo, brazil. *Data*, vol. 8, pp. 52, 2023.
[6] TeCSol. Rouen habitat s'associe à wind my roof et innove avec de l'électricité renouvelable sur les toits. Acesso em: 12 jul. 2024, 2022.
[7] C. e. a. Canuto. *Spectral Methods: Fundamentals in Single Domains.* Springer Berlin Heidelberg, ISBN 9783540307266, 2006.
[8] A. Nascimento, F. Mariano, E. Padilla, and A. Silveira-Neto. Comparison of the convergence rates between fourier pseudo-spectral and finite volume method using taylor-green vortex problem. *J Braz. Soc. Mech. Sci. Eng.*, vol. 42, pp. 1806–3691, 2020.
[9] A. RAO, M. THOMPSON, and T. LAWEKE. The flow past a circular cylinder translating at different heights above a wall. *Journal of Fluids and Structures*, pp. 1–13, 2013.
[10] A. HARICHANDAN and A. ROY. Numerical investigation of flow past single and tandem cylindrical bodies in the vicinity of a plane wall. *Journal of Fluids and Structures*, pp. 1–25, 2012.